3D/2D Model-to-Image Registration Applied to TIPS Surgery

Julien Jomier[1], Elizabeth Bullitt[2], Mark Van Horn[2], and Stephen R. Aylward[1]

[1] Computer-Aided Diagnosis and Display Lab, Department of Radiology
[2] Computer-Assisted Surgery and Imaging Laboratory, Department of Surgery
The University of North Carolina at Chapel Hill
27599 Chapel Hill, USA
julien@jomier.com, bullitt@med.unc.edu
mark_vanhorn@med.unc.edu, aylward@unc.edu

Abstract. In the context of image-guided TIPS (Transjugular, Intrahepatic, Portosystemic Shunt formation) surgery, the pose of a 3-dimensional model of the liver's vasculature is updated in real-time by tracking an ovoid balloon catheter. Therefore, it is critical to know the exact physical relationship between these objects prior to any real-time tracking. We have developed a new model-to-image registration technique which aligns a 3-dimensional model of the vasculature with two orthogonal fluoroscopic projections. Our technique is driven by the gradient information from the projection pairs at sample points along the centerlines of the model. Our algorithm shows speed, accuracy and consistency given clinical data.

1 Introduction

Endovascular surgery consists of inserting a catheter into a major artery or vein and guiding that catheter through a vascular network to a target region. The main difficulty with endovascular treatments is that the procedure is guided by two 2-dimensional projection fluoroscopic images which makes it difficult for the physician to visualize the needle and the target in 3D. Thus is especially true for TIPS surgery, since a contrast agent cannot be injected as the needle is advanced, the target, portal vein, is not visible when the needle is advanced through the liver from the hepatic vein. The goal of the computer-augmented TIPS project [5] is to provide a 3-dimensional visualization of the procedure to the surgeon and therefore improve accuracy and decrease the procedure time.

Before a TIPS procedure, a 3-dimensional model of the target vasculature is created from a previous CT/MR image using a ridge traversal technique [2]. During the procedure, the needle is tracked in real time [4] and the three-dimensional visualizations are provided by a stereo polarized projection display. However, because of breathing, needle pressure and heartbeat, the liver moves as the needle is guided through the target. Therefore, a real-time registration is performed by tracking an ovoid balloon catheter lodged in the liver parenchyma and its

movement is used to estimate the movement of the liver's vessels. In the context of this project, it is critical to define the actual position and orientation of the 3-dimensional vascular model, thus establishing the relationship of the balloon to the vasculature, prior to any tracking. In this paper, we describe a novel technique for 3D/2D model-to-image registration using tubular structures as the model. Some previous work on 3D/2D registration has been done by Liu [3] but that technique requires knowing the correspondences between the 3D and the 2D tubes to be aligned. On the other hand, Aylward et al. [1] have shown that tube-to-image registration is accurate and fast using 3-dimensional ultrasound data or magnetic resonance images without having to specify correspondences.

Figure 1 shows the 3-dimensional model of the vasculature before alignment and the two projection images.

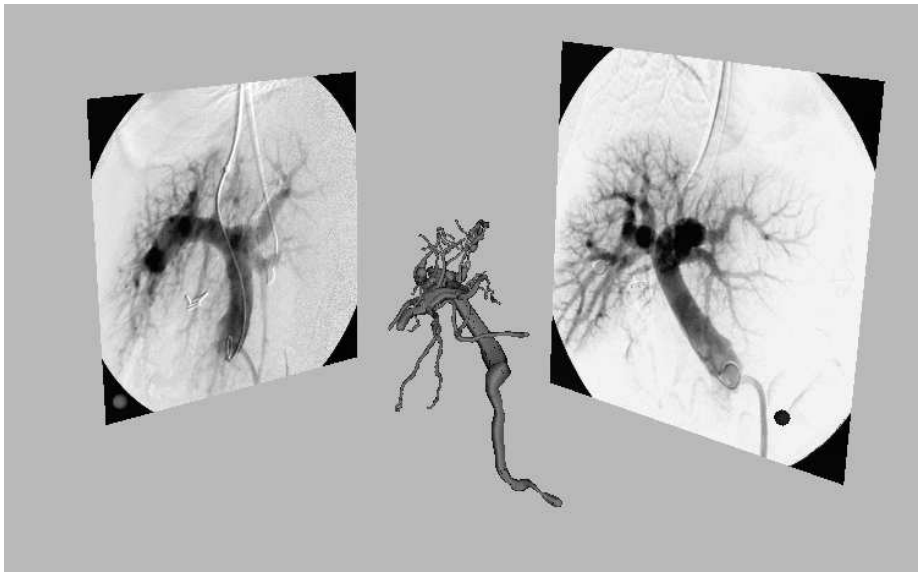

Fig. 1. System setup. 3-dimensional model of the vasculature is to be registered with two orthogonal fluoroscopic projections

2 Methods

2.1 Projection

We pre-process the pre-operative vascular model to enhance the speed and accuracy of the intra-operative registration. First, each tube of the 3-dimensional vasculature is sampled at a factor inversely proportional to the radius. This sampling produces a list of centerline points each having a radius and an orientation.

We choose to sample inverse proportionally to the radius since one can notice from figure 1 that the portal tree of the liver consists of a single major vein and a multitude smaller branches. Inverse proportional sampling allows the major vein to be registered with the same accuracy as the small branches. Second, during the registration process, each 3-dimensional sample point is projected onto the two images and its projected radius is also computed. We are following a standard perspective projection. A ray coming from the point source S intersects the object in X to project onto the plane P at x. The following equations give the relationship between X, x and the focal distance f.

$$f = \frac{S - P}{|X - S|} \tag{1}$$

$$x = S - P - (P - X) \cdot f \tag{2}$$

However, the projected radius is computed differently, since the projection of a 3-dimensional sphere onto a plane is reduced to an ellipse, we compute the average radius from the two maximum radii (one per direction). We pick two 3D points P_1 and P_2 on the sphere of radius R (and center C) that produces the maximum projected radius r_{max} such that $P_1 = C + (C - S)_\perp$ and $P_2 = C - (C - S)_\perp$. Then we project P onto the image using equation 2. Experiments show that this radius approximation gives a good radius estimation. We do not take into account any spherical distortion in the system. The source-to-film distance is high compared to the field of view and therefore the spherical distortion is limited. Experiments show that this assumption is valid for the x-ray system we use, however in the future we will add this parameter to the optimization process.

2.2 Registration

Our registration technique uses a gradient descent technique for several reasons. The first reason is that unreported experiments showed that the speed of the optimization can be significantly decrease by using this optimizer. However, it relies on the computation accuracy of the parameter's derivatives. The second reason deals with the separability of the parameters during the optimization. Optimizer that expects only one value as a metric, such as the 1+1 evolutionary optimizer [6], cannot deal with separable parameters. For optimizers such as gradient descent, the derivative vector drives the optimization process and the metric can easily tune each parameter independently. To solve our registration problem, we use a rigid body transform combined with a gradient descent optimizer and our gradient-based metric. From section 2.1 we project the 3D sample points of the model onto the image and we compute the gradient vector at a scale σ proportional to the projected radius. The anteroposterior projection I_{AP} contains valid information for the computation of the gradient in the X and Y direction and the lateral projection I_{LAT} in the Y and Z direction only. The following equations describe the derivatives of the parameters to be optimized.

$$\delta X = \frac{1}{N} \sum_{0}^{N} \nabla_\sigma(I_{AP}, x_{AP}) \tag{3}$$

$$\delta Y = \frac{1}{2N} \sum_{0}^{N} \nabla_\sigma(I_{AP}, y_{AP}) + \nabla_\sigma(I_{LAT}, y_{LAT}) \tag{4}$$

$$\delta Z = \frac{1}{N} \sum_{0}^{N} \nabla_\sigma(I_{LAT}, x_{LAT}) \tag{5}$$

$$\delta \alpha = \frac{1}{N} \sum_{0}^{N} \nabla_\sigma(I_{AP}, x_{AP}) \cdot N(x_{AP}) \tag{6}$$

$$\delta \beta = \frac{1}{2N} \sum_{0}^{N} \nabla_\sigma(I_{AP}, y_{AP}) \cdot N(y_{AP}) + \nabla_\sigma(I_{LAT}, y_{LAT}) \cdot N(y_{LAT}) \tag{7}$$

$$\delta \gamma = \frac{1}{N} \sum_{0}^{N} \nabla_\sigma(I_{LAT}, x_{LAT}) \cdot N(x_{LAT}) \tag{8}$$

with $x_{AP} = P(X, I_{AP})$ and $x_{LAT} = P(X, I_{LAT})$. N denotes the number of sample points from the 3-dimensional model. Contrary to the derivatives of the metric defined by Aylward [1], the gradient computation is not projected onto the normal of the tube. Also, the derivative computation might be imprecise if the alignment is far off; in that case, it might be interesting to use a different optimization strategy and use the match metric value instead of the gradient. In fact, the match metric value has a larger capture range and might be able to solve the registration problem. We also assume for now that the 3-dimensional model is approximately positioned in the middle of the projection system. This assumption will be released in the future since it does not always hold in the operating room. In some cases where the model is not perfectly located in the middle of the imaging system it is useful to include the magnification of the projected model as a translation part of the optimization. There are two approaches to solve the magnification problem. The first one is to maximize the sum of the Gaussian-blurred values of the projected sample points. The second approach deals with the computation of the derivative of the translation parameter. The latter, however, requires the model to be approximately aligned before computation.

We present, next, the plots of the derivatives from real datasets where the 3-dimensional model has been registered until convergence, then an offset of $\pm 10mm$ and an angle of $\pm 0.2rad$ was applied and the corresponding derivative values were reported. As one can see, X and Z derivatives are completely uncorrelated since we are using two different images for the computation. However, Y is correlated with X and Z as we can expect. Regarding rotation, derivative surfaces are smooth enough to perform a gradient descent optimization. The center of rotation is defined as the projection of the center of mass of the 3-dimensional vasculature.

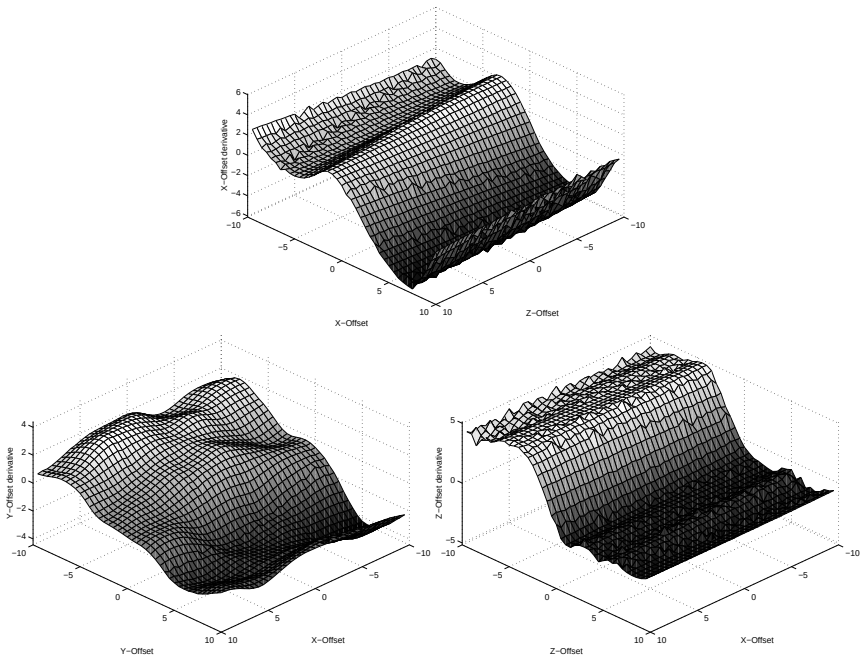

Fig. 2. Plots of the derivatives offset parameters. Note, axis are different

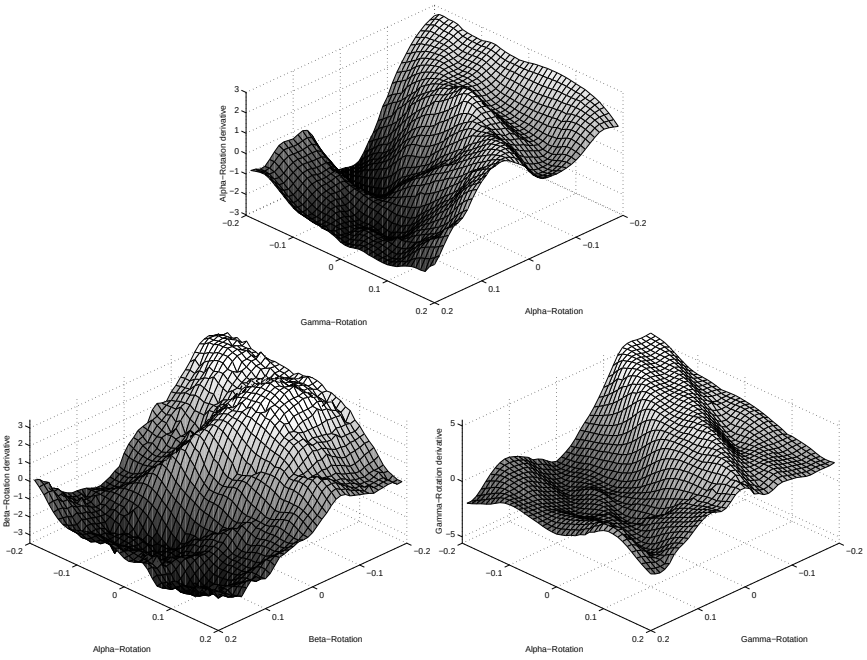

Fig. 3. Plots of the derivatives rotation angles parameters. Note, axis are different

3 Results

We conducted multiple experiments to evaluate the speed, robustness and accuracy of our algorithm on real datasets. Figure 4 shows the qualitative validation of our registration technique. For this experiment the extracted model is loaded directly in the scene using physical coordinates as well as the orientation of the patient. The field of view and the source-to-film distance are set using the values reported by the x-ray machine. Then the registration is performed without any manual intervention and is therefore fully automatic. Depending on the complexity of the 3D model and the sampling factor, the computation time can vary from 30 seconds up to 4 minutes. Prior to registration the 3-dimensional model of the vasculature can be pruned so that unnecessary blood vessels can be removed from the registration process. Also, a weighting factor can be applied on specific blood vessels which should be registered with high accuracy, for the moment the weighting factor is a positive linear function of the average radius of vessel.

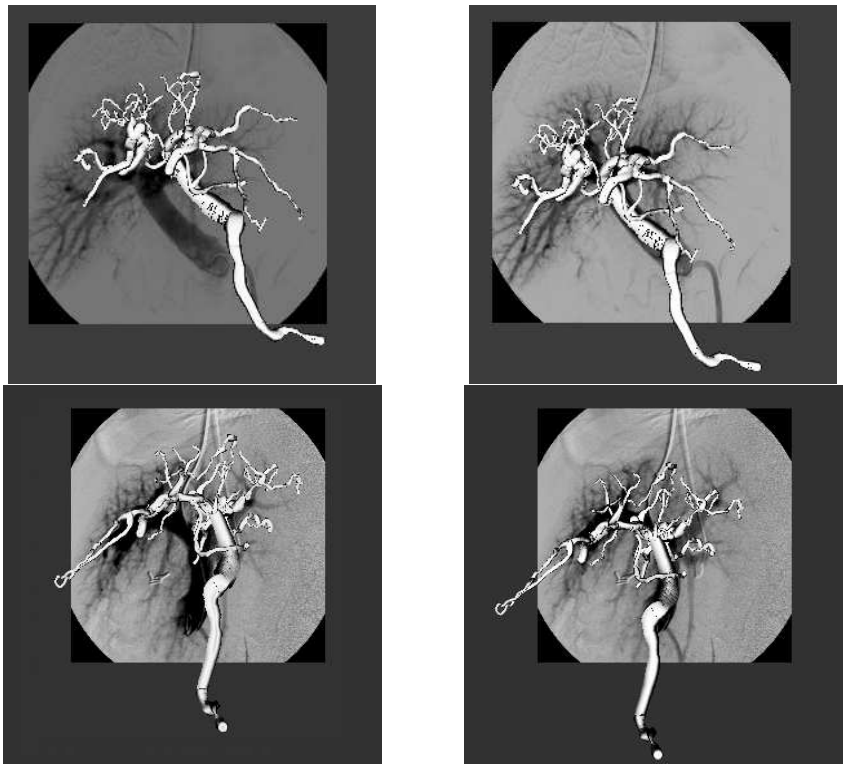

Fig. 4. Qualitative results of the 3D/2D registration. Vasculature before (left) and after registration (right) for both anteroposterior (top) and lateral (bottom) views

We conducted a Monte-Carlo validation experiment on real images. Figure 5 shows the resulting plots of this experiment. The vasculature was subsampled by a factor of 10 and 200 Monte-Carlo iterations were performed by adding random offsets and rotations after an initial registration. Our registration appears to be consistent even for large displacements ($\pm 10mm$) and rotation angles ($\pm 0.2rad$). The mean resulting displacement is $(X = -0.262, Y = -0.181, Z = -0.329)$ with corresponding standard deviations of $(X_\sigma = 0.62, Y_\sigma = 1.37, Z_\sigma = 0.54)$. The mean registered rotation is $(\alpha = 0.005, \beta = 0.009, \gamma = 0.01)$ with standard deviations of $(\alpha_\sigma = 0.080, \beta_\sigma = 0.033, \gamma_\sigma = 0.048)$. The registration is failing for some cases when the registration starts far from the solution. In fact, it can be the case for large offsets that only a part of the vasculature is inside of the image; this situation is not clinically viable during a TIPS procedure.

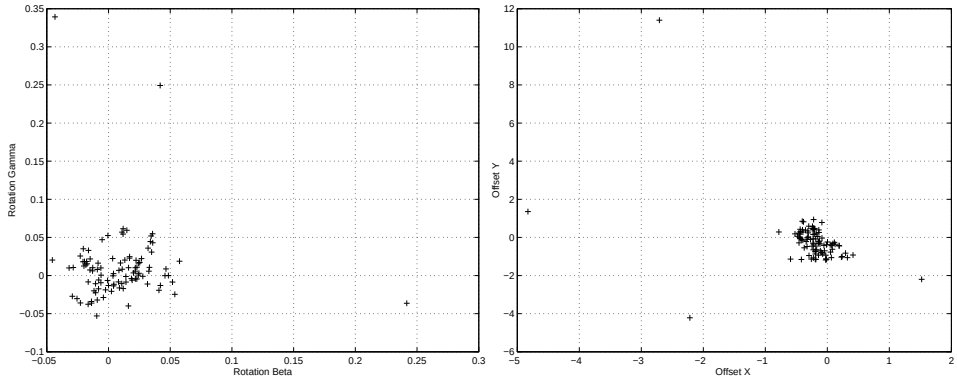

Fig. 5. Monte-Carlo experiments performed using 200 iterations and random offsets ranging between $\pm 10mm$ and random rotations between $\pm 0.2rad$

The registration runs in about two minutes without any speed optimization. We are confident that this registration time can be significantly decrease by tuning some of the parameters of the registration. Moreover, the algorithm can easily be parallelized.

4 Discussion and Conclusions

We have developed a new registration metric, which is driven by applying 3-dimensional derivatives to the parameters of two fluoroscopic projections images. Our technique does not require the specification of correspondences between blood vessel from the 3-dimensional model and their 2-dimensional projections. Our method shows excellent results on real datasets. We are currently extending the parameters space to estimating the relation between the projection planes. We are also performing validations using a phantom. Our software was implemented using the Insight Toolkit[7].

References

1. Aylward S, Jomier J, Weeks S, Bullitt E: Registration of Vascular Images International Journal of Computer Vision, November 2003, pages 15
2. Aylward S, Bullitt E: Initialization, Noise, Singularities, and Scale in Height-Ridge Traversal for Tubular Object Centerline Extraction IEEE Transactions on Medical Imaging, Feb, 2002, Pages 61-75
3. Liu A, Bullitt E, Pizer SM: 3D/2D registration using tubular anatomical structures as a basis MICCAI '98, Lecture Notes in Computer Science 1496: 952-963.
4. Jolly B, Van Horn M, Aylward S, Bullitt E: Needle tracking and detection in the TIPS endovascular procedure MICCAI 2003
5. Rosenthal M, Weeks S, Aylward S, Bullitt E, Fuchs H: Intraoperative tracking of anatomical structures using fluoroscopy and a vascular balloon catheter MICCAI 2001; Lecture Notes in Computer Science 2208: 1253-1254
6. Styner M, Gerig G: Evaluation of 2D/3D bias correction with 1+1ES optimiza-tion, Technical Report, BIWI-TR-179
7. The Insight Toolkit: National Library of Medicine Insight Segmentation and Registration Toolkit. http://www.itk.org

This work is funded in part by NIH-HLB R01 HL69808, the Whitaker Foundation (Aylward-RG-01-0341) and the National Library of Medicine's Insight Toolkit (ITK: Aylward-N01-LM-0-3501)

Further demos at caddlab.rad.unc.edu and jomier.com